Received: 25 October 2018 | Revised: 25 March 2019 | Accepted: 4 August 2019

DOI: 10.1111/jbi.13716

RESEARCH PAPER

Journal of Biogeography | WILEY

# Exploring rain forest diversification using demographic model testing in the African foam-nest treefrog *Chiromantis rufescens*

Adam D. Leaché[1] | Daniel M. Portik[2] | Danielle Rivera[3] | Mark-Oliver Rödel[4] | Johannes Penner[4,5] | Václav Gvoždík[6,7] | Eli Greenbaum[8] | Gregory F. M. Jongsma[9] | Caleb Ofori-Boateng[10,11] | Marius Burger[12,13] | Edem A. Eniang[14] | Rayna C. Bell[15] | Matthew K. Fujita[3]

[1]Department of Biology & Burke Museum of Natural History and Culture, University of Washington, Seattle, WA, USA

[2]Department of Ecology and Evolution, University of Arizona, Tucson, AZ, USA

[3]Department of Biology, The University of Texas at Arlington, Arlington, TX, USA

[4]Museum für Naturkunde, Leibniz Institute for Evolution and Biodiversity Science, Berlin, Germany

[5]Chair of Wildlife Ecology and Management, University of Freiburg, Freiburg, Germany

[6]Institute of Vertebrate Biology of the Czech Academy of Sciences, Brno, Czech Republic

[7]Department of Zoology, National Museum, Prague, Czech Republic

[8]Department of Biological Sciences, University of Texas at El Paso, El Paso, TX, USA

[9]Florida Museum of Natural History, University of Florida, Gainesville, FL, USA

[10]Forestry Research Institute of Ghana, Kumasi, Ghana

[11]Wildlife and Range Management Department, Kwame Nkrumah University of Science and Technology, Kumasi, Ghana

[12]African Amphibian Conservation Research Group, Unit for Environmental Sciences and Management, North-West University, Potchefstroom, South Africa

[13]Flora Fauna & Man, Ecological Services Ltd, Tortola, British Virgin Islands

[14]Department of Forestry and Wildlife, University of Uyo, Uyo, Nigeria

[15]Department of Vertebrate Zoology, National Museum of Natural History, Smithsonian Institution, Washington, DC, USA

**Correspondence**
Adam D. Leaché, Department of Biology & Burke Museum of Natural History and Culture, Seattle, WA, USA.
Email: leache@uw.edu

**Funding information**
German Ministry for Education and Research (BMBF), Grant/Award Number: 01LC0617J; German Science Foundation, Grant/Award Number: VE 183/4-1 and RO 306/1-2; Czech Science Foundation, Grant/Award Number: GACR 15-13415Y; Ministry of Culture of the Czech Republic, Grant/Award Number: 00023272; National Geographic Research and Exploration Grant, Grant/Award Number: 8556-08; National Science Foundation, Grant/Award Number: DEB-1145459; NIH, Grant/Award Number: S10 OD018174

Handling Editor: Krystal Tolley

## Abstract

**Aim:** Species with wide distributions spanning the African Guinean and Congolian rain forests are often composed of genetically distinct populations or cryptic species with geographic distributions that mirror the locations of the remaining forest habitats. We used phylogeographic inference and demographic model testing to evaluate diversification models in a widespread rain forest species, the African foam-nest treefrog *Chiromantis rufescens*.

**Location:** Guinean and Congolian rain forests, West and Central Africa.

**Taxon:** *Chiromantis rufescens*.

**Methods:** We collected mitochondrial DNA (mtDNA) and single-nucleotide polymorphism (SNP) data for 130 samples of *C. rufescens*. After estimating population structure and inferring species trees using coalescent methods, we tested demographic models to evaluate alternative population divergence histories that varied with respect to gene flow, population size change and periods of isolation and secondary contact. Species distribution models were used to identify the regions of climatic stability that could have served as forest refugia since the last interglacial.

  

**Results:** Population structure within *C. rufescens* resembles the major biogeographic regions of the Guinean and Congolian forests. Coalescent-based phylogenetic analyses provide strong support for an early divergence between the western Upper Guinean forest and the remaining populations. Demographic inferences support diversification models with gene flow and population size changes even in cases where contemporary populations are currently allopatric, which provides support for forest refugia and barrier models. Species distribution models suggest that forest refugia were available for each of the populations throughout the Pleistocene.

**Main conclusions:** Considering historical demography is essential for understanding population diversification, especially in complex landscapes such as those found in the Guineo–Congolian forest. Population demographic inferences help connect the patterns of genetic variation to diversification model predictions. The diversification history of *C. rufescens* was shaped by a variety of processes, including vicariance from river barriers, forest fragmentation and adaptive evolution along environmental gradients.

**KEYWORDS**

biogeography, demography, phylogeography, Rhacophoridae, SNPs, West Africa

## 1 | INTRODUCTION

The processes that generate and maintain high species diversity in tropical ecosystems are important contributors to global patterns of diversification (Jablonski, Roy, & Valentine, 2006; Pyron & Wiens, 2013). Understanding diversification processes is important for describing the composition of biodiversity, interpreting how ecosystems and biomes develop over time, and guiding decisions on how to preserve threatened biotas. In contrast to Pleistocene speciation observed in many temperate biomes, tropical species assemblages often have relatively deeper evolutionary origins extending into the Miocene (Moritz, Patton, Schneider, & Smith, 2000). Determining the ages of tropical taxa is important, because older lineages have more time for geographic, evolutionary and ecological mechanisms to influence species diversity. Many phylogenetic studies of reptiles and amphibians in tropical Africa support species-level diversification during the Miocene (Greenbaum, Portillo , Jackson, & Kusamba, 2015; Hughes, Kusamba, Behangana, & Greenbaum, 2017; Larson, Castro, Behangana, & Greenbaum, 2016; Menegon et al., 2014; Portillo et al., 2018), although there are also examples of more recent diversification in the Pliocene and Pleistocene in amphibians (Bell et al., 2017; Jongsma et al., 2018), lizards (Leaché et al., 2017), birds (Fjeldså & Bowie, 2008), mammals (Gaubert et al., 2016) and even rainforest trees (Hardy et al., 2013).

The Guinean and Congolian rain forests of West and Central Africa are the centres of biological diversity with considerable endemism (Myers, Mittermeier, Mittermeier, Fonseca, & Kent, 2000; Plana, 2004; White, 1979). Three major models of tropical species diversification proposed for the region include the forest refugia, riverine barrier and ecotone models (Myers et al., 2000; Plana, 2004; White, 1979). The long and complex history of the Guineo–Congolian rain forest has produced phylogeographic patterns within species that fit multiple models (Portik et al., 2017). For example, the genetic structure of forest-restricted species often matches both the locations of forest refugia and the divisions created by major river barriers (Barej et al., 2011; Gonder et al., 2011; Leaché & Fujita, 2010; Marks, 2010; Penner, Augustin, & Rödel, 2017), making it difficult to characterize diversification mechanisms using phylogeographic patterns alone.

Diversification models can be explored in more detail by contrasting their distinctive geographic and demographic predictions (Moritz et al., 2000). The forest refugia model predicts that rain forest expansions and contractions result in population fragmentation and cyclical shifts in population size, and that these periods of divergence in allopatry may ultimately lead to speciation. Aridification cycles during the Pleistocene caused cyclical contractions and expansions of rain forest throughout West and Central Africa (Dupont, Jahns, Marret, & Ning, 2000; Hamilton & Taylor, 1991; Maley, 1991; Salzmann & Hoelzmann, 2005), and the Upper and Lower Guinean Forest Blocks are currently divided by the Dahomey Gap (Figure 1), an arid savanna corridor that extends from Ghana to Nigeria and acts as a major biogeographic barrier for forest taxa (Dupont et al., 2000; Hamilton & Taylor, 1991; Maley, 1991; Salzmann & Hoelzmann, 2005). Dry forests and savannas are effective isolating barriers for rain forest frogs (Penner et al., 2013). By contrast, the riverine barrier model predicts that populations bisected by major rivers will diverge in allopatry without population size fluctuations. Rivers are important barriers for several species of African forest frogs (Charles et al., 2018; Jongsma et al., 2018; Portik et al., 2017). Finally, the ecotone model predicts parapatric speciation along an environmental gradient with isolation by distance and divergence with gene flow. Accurately distinguishing among these models requires an

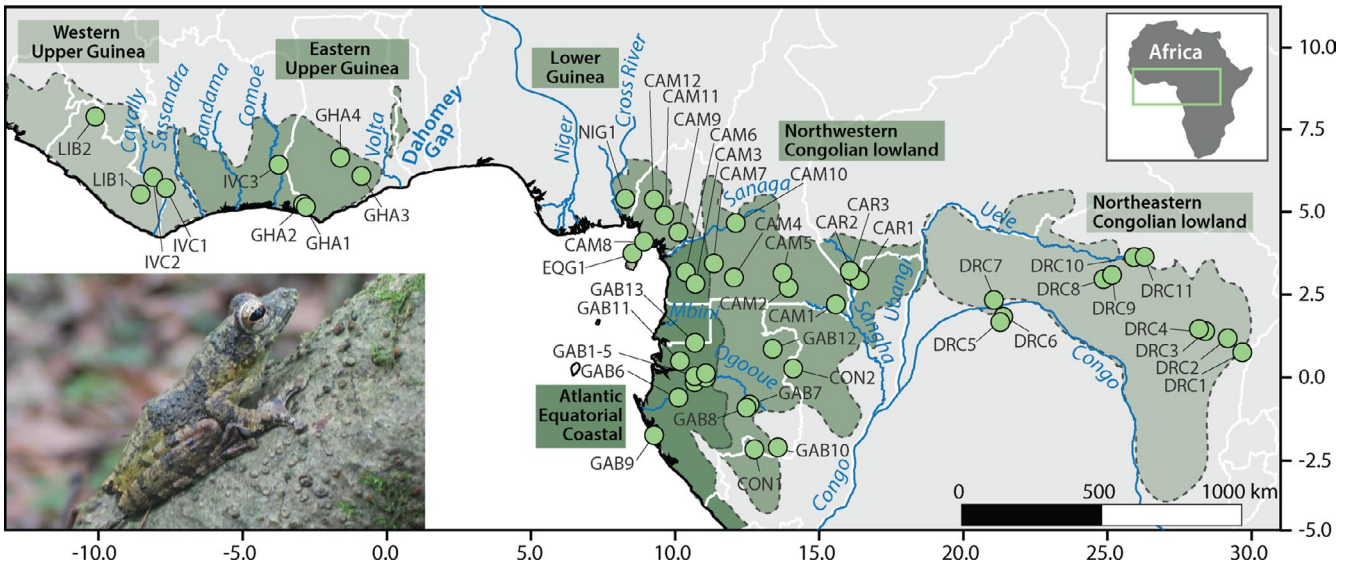


**FIGURE 1** Distribution of the sampled populations of *Chiromantis rufescens* in West and Central Africa, and the locations of major rivers and forests. Photograph of *C. rufescens* from Atewa Hills, Ghana

integrative approach that combines phylogeographic inference, historical demography and species distribution modelling (Barratt et al., 2018; Charles et al., 2018; Portik et al., 2017).

The African foam-nest treefrog *Chiromantis rufescens* (Günther, 1869) is distributed throughout the major Guinean and Congolian forest blocks scattered from Guinea to Uganda where it occurs in tropical and subtropical moist broadleaf forest ecoregions (Olson & Dinerstein, 2002) and adjacent degraded habitats. The genus *Chiromantis* contains 19 species with distributions in tropical Asia (15 species) and Africa (4 species; Li et al., 2009; Meegaskumbura et al., 2015; Onn, Grismer, & Brown, 2018; Yu, Rao, Zhang, & Yang, 2009). Divergence dating analyses suggest that the common ancestor of African *Chiromantis* may have colonized from Asia during the Oligocene or Eocene (33–51 Myr; Vences et al., 2003), or as early as the Miocene (Yuan et al., 2019). The divergence time between *C. rufescens* and its closest relative, the African grey treefrog (*C. xerampelina*) is currently unknown, but the expansive distribution of *C. rufescens* across the Dahomey Gap and all major forested areas and riverine barriers in West and Central Africa (Penner et al., 2017; Penner, Wegmann, Hillers, Schmidt, & Rödel, 2011) suggests a pre-Pleistocene origin. In addition, *C. rufescens* occurs on Bioko Island, a land bridge island in the Gulf of Guinea that was connected to the mainland during the last glaciation (Lee, Halliday, Fitton, & Poli, 1994), adding island colonization as another potential source of diversification in this widespread species (Bell et al., 2017; Charles et al., 2018; Leaché & Fujita, 2010).

*Chiromantis rufescens* is a unique member of the Guineo–Congolian rain forests that is characterized by a reproductive strategy that is unique among the remaining frog fauna in West and Central African rain forests. *Chiromantis rufescens* time their reproduction with the rainy season, and breed by producing foam nests that are attached to vegetation above seasonal ponds or puddles, and tadpoles drop from the foam nest and into the water 5–8 days later, presumably benefitting from a temporary reduction in tadpole mortality while evading aquatic predators (Coe, 1967, 1974), although some terrestrial predators have learned to harvest this protein source (Rödel, Range, Seppänen, & Noë, 2002). The reliance of the species on primary and secondary rain forest has resulted in a fragmented distribution throughout much of the region. Dispersal appears to be limited, since they are restricted to forested regions. As a consequence of breeding and placing their foam nests above lentic water, they appear to avoid the main courses of large rivers, which are potentially strong dispersal barriers.

In cases where species have colonized West Africa, particularly from East Africa or even Asia, an emerging pattern is that deep genetic divisions are not found between the Guinean and Congolian forests, but are instead located much further west within the Upper Guinean forest (Barej et al., 2014; Dowell et al., 2016; Jongsma et al., 2018; Zimkus et al., 2017). Whether the population structure and phylogeographic history of *C. rufescens* matches the pattern observed in other colonizers from Asia with deep genetic divergences in the Upper Guinean forest is currently unknown. Ultimately, determining which taxa share concordant spatial and temporal genetic breaks within the Upper Guinean forest will clarify the evolutionary origins of this unique forest fauna, and more generally, will enable us to characterize the history of faunal exchange between Africa and Asia.

In this study, we investigate the diversification history of *C. rufescens* using phylogeographic inference, demographic model testing and ecological modelling. Phylogeographic inference is used to determine the relationships among populations, and to estimate their divergence times. The demographic model testing framework is important for discriminating among alternative diversification models that may explain the contemporary spatial distributions of populations and their patterns of genetic diversity. Ecological

modelling is used to identify areas of long-term climate stability that could have served as refugia since the Last Interglacial. Our study has two specific goals: (a) test whether *C. rufescens* fits the emerging pattern observed in other colonizers of West Africa by supporting a deep genetic break within the Upper Guinean forest, and (b) characterize the roles of barriers, forest refugia and ecotones in the diversification of *C. rufescens*.

## 2 | MATERIALS AND METHODS

### 2.1 | Sampling

A total of 130 samples of *C. rufescens* were collected from throughout West and Central Africa (Figure 1). Nearly half of the collecting sites are represented by a single sample, and the average number of samples per site is 2.5 (Table 1). Specimen voucher information and locality data are provided in Table S1.

### 2.2 | Genetic data

We sequenced a 546 base pair portion of the mtDNA 16S ribosomal RNA gene (16S) using primers 16SA and 16SB (Palumbi, 1996). The sequences were edited using Geneious 11.1 and aligned with MAFFT 5 (Katoh, Kuma, Toh, & Miyata, 2005) with the E-INS-I algorithm. The 16S sequences are deposited in GenBank (accession numbers: MK789304–MK789428).

We collected SNP data following the ddRADseq protocol (Peterson, Weber, Kay, Fisher, & Hoekstra, 2012). Our library preparation methods are similar to those used in other studies of African frog phylogeography (Charles et al., 2018; Portik et al., 2017). Briefly, we double-digested DNA using the restriction enzymes SbfI and MspI, followed by bead purification and ligation of barcoded Illumina adaptors, size-selection and library quantification. Samples were sequenced on a single Illumina HiSeq 4000 lane (50-bp, single-end reads) at the QB3 Genome Sequencing facility at the University of California, Berkeley.

We processed raw Illumina reads using the program 'iPyRad' 0.7.13 (Eaton, 2014). We clustered the filtered reads for each sample using the program VSEARCH 1.1.0 (Edgar, 2010) using a clustering threshold of 90%. We removed consensus sequences that had low coverage (<6 reads), excessive undetermined or heterozygous sites (>8), too many alleles for a sample (>2 for diploids), and an excess of shared heterozygosity among samples (paralog filter = 0.5). For the final SNP alignment, we removed loci and samples with ≥50% missing data. We randomly selected one SNP per locus for species tree inference and demographic analyses.

### 2.3 | Population structure

To estimate the number of populations, we used discriminant analysis of principal components (DAPC) implemented in the R package ADEGENET (Jombart & Ahmed, 2011; Jombart, Devillard, & Balloux, 2010). We used the *find.clusters* function to evaluate *K* (number of

**TABLE 1** Samples of *Chiromantis rufescens* sequenced using ddRADseq

| Country | Label | GPS coordinate | *n* |
|---|---|---|---|
| Cameroon | CAM1 | 2.1388, 15.6557 | 3 |
| Cameroon | CAM2 | 2.6445, 14.0312 | 5 |
| Cameroon | CAM3 | 2.7795, 10.8258 | 2 |
| Cameroon | CAM4 | 2.9622, 12.1521 | 2 |
| Cameroon | CAM5 | 3.0881, 13.8268 | 1 |
| Cameroon | CAM6 | 3.1336, 10.4939 | 5 |
| Cameroon | CAM7 | 3.3913, 11.4663 | 2 |
| Cameroon | CAM8 | 4.0683, 9.0689 | 2 |
| Cameroon | CAM9 | 4.3394, 10.2450 | 1 |
| Cameroon | CAM10 | 4.6116, 12.2254 | 3 |
| Cameroon | CAM11 | 4.8498, 9.7718 | 4 |
| Cameroon | CAM12 | 5.3372, 9.4173 | 2 |
| Central African Republic | CAR1 | 2.8600, 16.4700 | 1 |
| Central African Republic | CAR2 | 2.9252, 16.2546 | 3 |
| Central African Republic | CAR3 | 2.9854, 16.2325 | 6 |
| Democratic Republic of the Congo | DRC1 | 0.6823, 29.6513 | 2 |
| Democratic Republic of the Congo | DRC2 | 1.1050, 29.1496 | 1 |
| Democratic Republic of the Congo | DRC3 | 1.3938, 28.6176 | 1 |
| Democratic Republic of the Congo | DRC4 | 1.3975, 28.5234 | 2 |
| Democratic Republic of the Congo | DRC5 | 1.6737, 21.4099 | 1 |
| Democratic Republic of the Congo | DRC6 | 1.7483, 21.4202 | 8 |
| Democratic Republic of the Congo | DRC7 | 2.2559, 21.0971 | 3 |
| Democratic Republic of the Congo | DRC8 | 2.8823, 24.8691 | 1 |
| Democratic Republic of the Congo | DRC9 | 3.0083, 25.1652 | 1 |
| Democratic Republic of the Congo | DRC10 | 3.5471, 25.9115 | 2 |
| Democratic Republic of the Congo | DRC11 | 3.5566, 26.2873 | 1 |
| Equatorial Guinea | EQG1 | 3.7111, 8.6666 | 6 |
| Gabon | GAB1 | −0.0009, 11.1662 | 1 |
| Gabon | GAB2 | −0.0029, 10.7814 | 1 |
| Gabon | GAB3 | −0.0492, 11.1643 | 1 |
| Gabon | GAB4 | −0.1750, 10.7814 | 1 |
| Gabon | GAB5 | −0.1848, 10.7773 | 3 |
| Gabon | GAB6 | −0.6410, 10.2177 | 1 |
| Gabon | GAB7 | −0.8683, 12.6724 | 1 |

(Continues)

**TABLE 1** (Continued)

| Country | Label | GPS coordinate | *n* |
|---|---|---|---|
| Gabon | GAB8 | −0.8799, 12.6549 | 2 |
| Gabon | GAB9 | −1.7710, 9.3694 | 1 |
| Gabon | GAB10 | −2.1567, 13.6346 | 1 |
| Gabon | GAB11 | 0.4536, 10.2781 | 2 |
| Gabon | GAB12 | 0.8071, 13.4723 | 7 |
| Gabon | GAB13 | 1.0027, 10.7994 | 2 |
| Ghana | GHA1 | 5.2818, −2.6417 | 5 |
| Ghana | GHA2 | 5.2902, −2.6396 | 2 |
| Ghana | GHA3 | 6.1280, −0.6289 | 6 |
| Ghana | GHA4 | 6.6870, −1.3441 | 1 |
| Ivory Coast | IVC1 | 5.8361, −7.3493 | 6 |
| Ivory Coast | IVC2 | 6.1672, −7.7883 | 1 |
| Ivory Coast | IVC3 | 6.4986, −3.4674 | 1 |
| Liberia | LIB1 | 5.6564, −8.2202 | 3 |
| Liberia | LIB2 | 8.0337, −9.7357 | 1 |
| Nigeria | NIG1 | 5.36390, 8.43341 | 4 |
| Republic of the Congo | CON1 | −2.2103, 12.8253 | 3 |
| Republic of the Congo | CON2 | 0.2099, 14.1754 | 2 |

populations) values between 1 and 10 using the Bayesian information criterion (BIC), and selected the *K* value with the lowest BIC score. We used the *opt.pca* function to optimize the number of principal components to retain, and then generated a DAPC scatterplot of genetic variation and a barplot showing the membership probabilities and population composition. For two neighbouring populations that were only weakly differentiated, we tested for isolation by distance (IBD) using Mantel tests in ADEGENET. We calculated Nei's genetic distances (Nei, 1978) between sample locations and conducted Mantel tests with geographic distances to test for a continuous cline of genetic differentiation versus two distinct and differentiated populations.

We also estimated population structure using the likelihood-based method STRUCTURE 2.3 (Pritchard, Stephens, & Donnelly, 2000). We used the admixture model with correlated allele frequencies without treating sampling locations as prior information. The program was run with a burn-in of 50,000 iterations, followed by 500,000 MCMC steps. Each value of *K* between 1 and 10 was run five times. Replicate runs of each *K* value were combined using the program CLUMPP (Rosenberg, 2004) and visualized with DISTRUCT v1.1 (Rosenberg, 2004). To select the optimal value of *K*, we used the delta *K* values from STRUCTURE HARVESTER (Earl & vonHoldt, 2012).

We calculated pairwise $F_{ST}$ values (Weir & Cockerham, 1984) among the inferred populations using 'VCFtools' v0.1.15 (Danecek et al., 2011). We quantified the partitioning of genetic variation within and among populations with a hierarchical analysis of molecular variance (AMOVA) using the program 'GENODIVE' v2.0b27 (Meirmans & Van Tienderen, 2004). Significance was assessed using 1,000 permutations, and missing data were replaced with randomly drawn alleles based on overall population frequencies. To evaluate the influence of river barriers and major forest block fragmentation on genetic variation, we partitioned the populations into three different higher level groups to find the population grouping that maximized the among-group variation. These groupings each included two partitions: (a) opposite sides of the Dahomey Gap (equivalent to opposite sides of the Cross River), (b) opposite sides of the Sanaga River and (c) divergence within the Upper Guinean forest between the Western and Eastern Upper Guinea forest ecoregions.

## 2.4 | Species tree estimation

We estimated a species tree from the SNP data using SNAPP 1.4.0 (Bryant, Bouckaert, Felsenstein, Rosenberg, & RoyChoudhury, 2012) implemented in BEAST 2.5.0 (Bouckaert et al., 2014). For sample partitioning, we used the population assignments estimated using STRUCTURE and ADEGENET. To increase the number of shared SNPs among populations and to expedite the analysis, we assembled a SNP matrix containing a reduced number of samples for each population (five samples per major forest region), and used samples with high data coverage representing different geographic areas. The mutation rates *u* and *v* were set to 1.0, and the species tree prior used the default setting (improper 1/X distribution). We set the prior for the expected genetic divergence theta ($\theta$) using a gamma distribution $\theta \sim G(2, 100)$ with a mean of alpha/beta = 0.02. The analysis was run for 1,000,000 iterations sampling every 100 steps and discarded the first 25% as burn-in. We ran the analysis twice using different random starting seeds to check for stable parameter estimation as a sign of convergence. The posterior probability distribution of species tree topologies was visualized using DENSITREE (Bouckaert, 2010).

Obtaining a species tree with branch lengths converted to units of time is important for placing lineage diversification into a biogeographic perspective. However, we currently lack robust estimates for genome-wide mutation rates in frogs to date divergence times on SNP phylogenies. One potential solution is to use human rate estimates as a rough approximation, and to calculate divergence times by dividing the estimated branch lengths by the human nuclear mutation rate of $1 \times 10^{-8}$ (Lynch, 2010; Scally & Durbin, 2012). Although this same approach has provided reasonable results for other African frogs that were consistent with divergence estimates obtained using mtDNA and traditional substitution rate assumptions (Charles et al., 2018; Portik et al., 2017), the magnitude of inaccuracy associated with this rate calibration is unknown. To obtain an independent estimate of divergence times, we conducted a time-calibrated phylogenetic analysis of the mtDNA 16S data using secondary fossil calibrations (see below).

The species tree for the 16S mtDNA sequences was estimated using 'StarBEAST2' (Ogilvie, Bouckaert, & Drummond, 2017). Although not widely appreciated, single-gene analyses using the multispecies coalescent are advantageous, because they can provide information about incomplete lineage sorting and more accurate estimates of topological uncertainty and divergence times (Ogilvie et al., 2017). The population assignments matched those

used for analysis of the SNP data, with the exception of allowing for two groups within the LGC forest to account for their lack of monophyly. We time calibrated the species tree using two secondary calibration points from Vences et al. (2003), including a 32 Ma divergence between *Chiromantis* and *Polypedates*, and a 60 Ma divergence between Rhacophoridae and *Amnirana galamensis*. Priors were implemented on the species tree topology (yule tree prior) using normal distributions with standard deviations = 1.0. We included sequences from additional species of *Chiromantis* and other outgroups from GenBank, including *C. doriae* (MG935758), *C. petersii* (GQ204733), *C. xerampelina* (AF215348), *Polypedetes cruciger* (AF215357) and *A. galamensis* (AY322303). The analysis implemented an uncorrelated lognormal clock (estimating the clock rate), analytical population size integration and gene ploidy = 0.5 for haploid and uniparentally inherited mtDNA. The HKY substitution model (Hasegawa, Kishino, & Yano, 1985) with gamma-distributed rate variation was selected using the Bayesian information criterion after analysing the *C. rufescens* sequences with 'JModelTest' 2.1.3 (Darriba, Taboada, Doallo, & Posada, 2012). The analysis was run for 100,000,000 iterations sampling every 10,000 steps and discarded the first 10% as burn-in. We ran the analysis twice using different random starting seeds to check for stable parameter estimation as a sign of convergence. The posterior probability distribution of species tree topologies was visualized using 'DensiTree'. A maximum clade credibility tree for the 16S gene tree (estimated jointly with the species tree) was summarized using 'TreeAnnotator'.

## 2.5 | Demographic models

To test alternative demographic models describing the diversification of *C. rufescens* in the Guinean and Congolian forests, we simulated the two-dimensional (2D) joint site frequency spectrum (JSFS) of genetic variation between populations using Moments (Jouganous, Long, Ragsdale, & Gravel, 2017). Moments uses differential equations to simulate the evolution of allele frequency distributions over time and is closely related to the diffusion approximation method used in the program ∂a∂i (Gutenkunst, Hernandez, Williamson, & Bustamante, 2009).

We optimized 20 demographic models (Figure S1) that focus on aspects of historical demography that are important for models of African rain forest diversification, mainly divergence with gene flow and/or population size changes (Barratt et al., 2018; Charles et al., 2018; Portik et al., 2017). The models make different predictions concerning geographic modes of speciation, types of isolating barriers and evolutionary mechanisms following divergence. For example, allopatric speciation (= river barrier model) and parapatric speciation (= ecotone model) either exclude or include post-divergence gene flow, respectively. For the forest refugia model, population size change is expected to occur following population divergence, since population trajectories should be directly influenced by changes in forest sizes through time. The simplest models include divergence with no gene flow, divergence with symmetric gene flow, or divergence with asymmetric gene flow. Additional complexity is added to each of these models by including an instantaneous population size change event, and additionally, by restricting gene flow to either the period following divergence (ancient migration) or the period following the size change event (secondary contact). The most complex models allow for population size change and variable migration across two or three discrete time intervals (= epochs).

We compared 2D demographic modelling for population pairs that were selected using either geographic or phylogenetic criteria. The geographic comparisons tested population pairs with neighbouring distributions that have the potential for gene flow. Alternatively, phylogenetic comparisons used the species tree topology to ensure that only sister pairs of populations were tested. Due to the asymmetric shape of the species tree, the phylogenetic comparisons required populations to be combined together to test divergence events deeper in the species tree.

Outgroup sequence information was unavailable for 2D models, and we therefore used folded JSFS. To maximize the number of segregating sites used in analyses, populations were projected down to smaller sample sizes. Four rounds of model optimization were performed using the log_lbfgsb optimizer (Jouganous et al., 2017). Each round of model optimization used 100 replicate searches and 100 iterations per step, and a multinomial approach to estimate the log likelihood of each model. The parameters from the best-scoring replicate were used as starting values for the next round of optimization. After the final round of optimization, the replicate with the highest likelihood for each model was used to calculate AIC scores, ΔAIC scores, and Akaike weights (wAIC; Burnham & Anderson, 2003). Replicate analyses were conducted to ensure that the optimization routine was stable. Python scripts for performing model fitting and execute plotting functions are available at github.com/dportik/moments_pipeline.

## 2.6 | Species distribution modelling

To build a species distribution model (SDM) for *C. rufescens*, we compiled samples used for genetic analysis with all museum locality information available online using the vertnet data portal (Constable et al., 2010), which provided a total of 302 georeferenced specimen records. We estimated an SDM using Maxent (Phillips, Anderson, & Schapire, 2006), implemented in 'SdmToolbox' v2.2 (Brown, 2014; Brown, Bennett, & French, 2017), We utilized the "remove highly correlated variables" function to remove variables with a Pearson's correlation coefficient more than 0.75, which resulted in the use of eight bioclimatic layers, elevation, vegetation height and distance to rivers (Farr et al., 2007; Hijmans, Cameron, Parra, Jones, & Jarvis, 2005; Penner et al., 2017; Roll, Geffen, & Yom-Tov, 2015; Simard, Pinto, Fisher, & Baccini, 2011). To choose optimal model parameters, we evaluated five combinations of feature classes, including linear, linear + quadratic, hinge, linear + quadratic + hinge and linear + quadratic + hinge + product + threshold. We varied the regularization multipliers from 0.5 to 5, in increments of 0.5 and ran jackknifing to measure the variable importance. We then selected the model that

had the lowest test omission (low omission rate), highest discrimination ability (high area under the curve, AUC) and least complexity (Brown, 2014; Radosavljevic & Anderson, 2014; Shcheglovitova & Anderson, 2013). We used three methods to reduce the effects of spatial autocorrelation and overfitting; (a) a 100-km buffer around each occurrence record was used to sample background data (using a minimum convex polygon), (b) specimen occurrence records were spatially rarefied (10-km distance between samples) resulting in 83 unique localities and (c) records were partitioned for background testing and training (Boria, Olson, Goodman, & Anderson, 2014; Hijmans, 2012; Veloz, 2009). To estimate the areas of potential stability, we tested and trained models using the eight bioclimatic layers from the previous analysis to ascertain optimal parameters, projected models to past climate data from the mid-Holocene (6 kybp), the last glacial maximum (LGM; 21 kybp) and the last interglacial (LIG; 120 kybp), and overlaid the resulting maps to identify shared areas of occurrence (Devitt, Devitt, Hollingsworth, McGuire, & Moritz, 2013; Yannic et al., 2014).

## 3 | RESULTS

### 3.1 | Genetic data

The final 16S mtDNA alignment for *C. rufescens* is 544 bp and includes 125 sequences with 54 variable sites. Nine samples were dropped from the ddRADseq dataset to maintain a high level of data completeness, resulting in 121 samples with at least 50% data presence. The average coverage per sample was 29.2× (Table 2; Table S2). The final SNP assembly used for population structure inference contained 6,994 SNPs. The reduced dataset used for phylogenetic inference contained 1,390 SNPs. Population-level assemblies used for demographic model testing contained 429 to 6,360 loci (Table S3). The demultiplexed ddRADseq data are deposited at the NCBI SRA (PRJNA528800).

### 3.2 | Population structure

A summary of the population structure and phylogeographic patterns found within *C. rufescens* based on SNP data is provided in Figure 2. The population structure estimation using DAPC and STRUCTURE both support the $K = 5$ model, with the locations of the inferred populations coinciding geographically with the following major forest blocks: (a) Western Upper Guinean (UGW), (b) Eastern Upper Guinean (UGE), (c) Lower Guinean forest (LG), (d) Congolian forest, primarily Northeastern Congolian lowland forest (CON) and (e) a broadly distributed population (LGC) spanning the Atlantic Equatorial Coastal forest (AEC) in Lower Guinean and the North-western Congolian lowland forests (NWC) in the Congolian lowland forest (Figure 2a-c; Table S4, Figure S2). The $K = 6$ model, which has a BIC score that is nearly identical to the $K = 5$ model, further subdivides the LGC population into two groups that correspond roughly to the AEC and NWC forests, but the genetic variation among these populations is largely overlapping (Figure 2c; Figure S3), and they co-occur geographically near the Ogooué River in Gabon (Figure 2b). A test for IBD within the LGC population, which includes the AEC and NWC forests, was significant ($P = .001$; Figure S4). Further population structure is supported within the CON population, some of which is associated with variation on opposite sides of the Congo River and with the easternmost populations ($K = 3$; Figure S5). Additional structure is also supported within the LG population ($K = 2$) between Nigeria and the remaining locations, which cluster Bioko Island together with samples from Cameroon (Figure S5). In general, the SNP data are able to differentiate each unique collecting locality when using sample localities as pre-defined groupings (Figure S5).

Pairwise $F_{ST}$ values range from 0.025 to 0.405 with significant $p$ values < .001 (Table 3). The pairwise comparisons including the population in the Western Upper Guinean forest (UGW) provided large $F_{ST} > 0.14$ (Table 3). The $F_{ST}$ value for the comparison between the populations within the LGC (AEC and NWC) was the smallest ($F_{ST} = 0.025$; Table 3), further supporting these populations as only weakly differentiated. Among-population average pairwise sequence divergence of 16S ranged from 2.6% to 3.2% for comparisons with UGW, while the lowest level of sequence divergence of 1.3% was between UGE and LG (Table 3). AMOVA results indicate the presence of hierarchical population structure between all groups tested ($p < .005$; Table 4). Among group variation ($F_{ST}$) was lowest across the Sanaga River (11.0%), followed by the Dahomey Gap/Cross River (17.8%; Table 4). The proportion of variation produced from differences among groups was maximized (30.9%) by dividing the populations within the Upper Guinean forest (Table 4).

**TABLE 2** Summary of the ddRADseq data assembly for 121 *Chiromantis rufescens* samples. Missing data thresholds required at least 50% data presence for each locus and sample

| Variable | Mean | Min | Max |
|---|---|---|---|
| Reads passing filters | 3,539,479 | 511,520 | 20,110,021 |
| Clusters | 115,873 | 36,143 | 406,977 |
| Heterozygosity | 0.0170 | 0.0136 | 0.0201 |
| Error | 0.0032 | 0.0019 | 0.0067 |
| Coverage | 29.2 | 12.0 | 69.3 |
| Assembled loci | 4,992 | 1,870 | 6,639 |

### 3.3 | Species tree estimation

The species tree topology estimated using the SNP data in SNAPP provides strong support for all relationships (posterior probabilities = 1.0; Figure 2). The species tree does not provide support for the monophyly of the Upper Guinean populations (UGW + UGE) or the Guinean versus Congolian forests. Instead, the initial divergence in the species tree separates the Western Upper Guinean (UGW) population from all others, followed by the divergence of the Congolian (CON) population (Figure 2). Using a mutation rate calibration assumption for the SNP data, the root

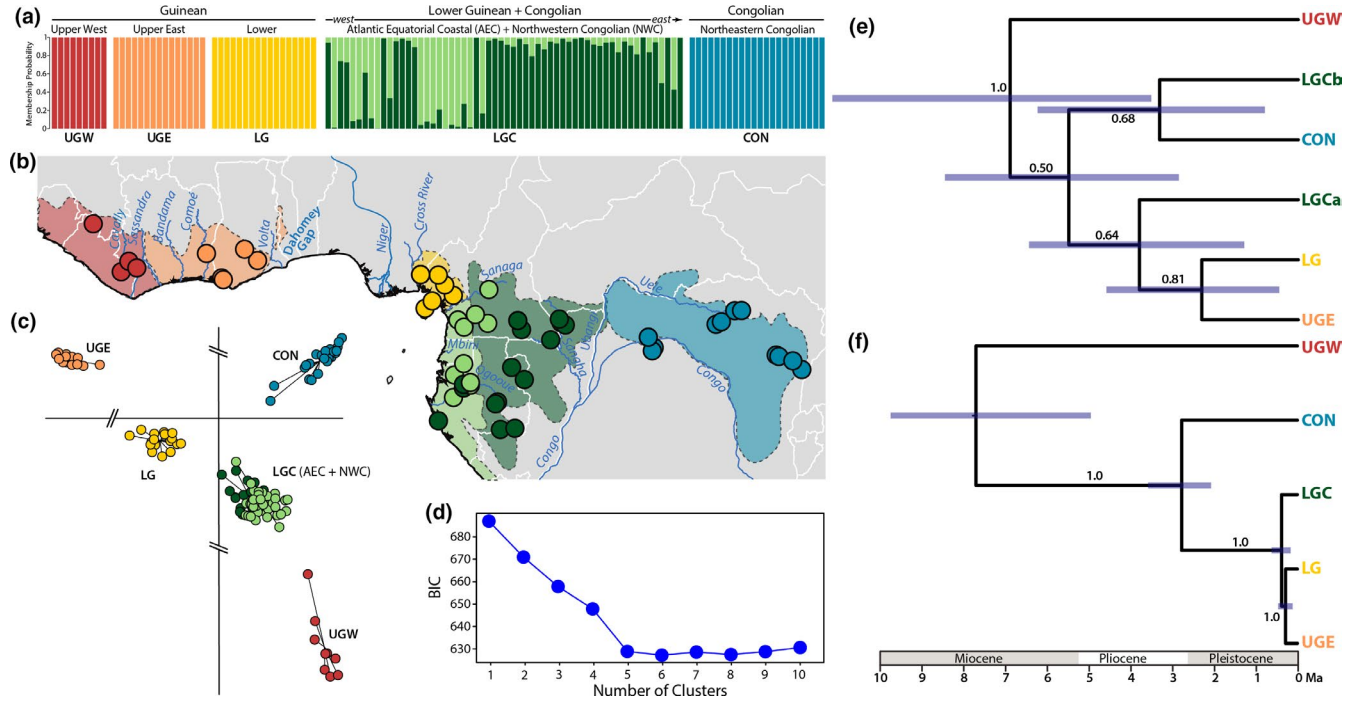


**FIGURE 2** Population structure and phylogeographic patterns within *Chiromantis rufescens*. (a) Barplot showing membership probabilities under the $K = 6$ model. Under the $K = 5$ model, the LGC populations are combined. (b) Geographic distributions of the six populations. (c) DAPC scatterplot for the $K = 6$ model. The AEC and NWC populations are overlapping. (d) Inference of the number of populations using the Bayesian information criterion (BIC). (e) Species trees estimated using the 16S mtDNA data analysed in StarBEAST2. (f) 1,390 SNPs analysed in Snapp. Posterior probability values are shown on branches, and the divergence times (mean and 95% highest posterior density, HPD) are shown as node bars

**TABLE 3** Measures of genetic variation among populations of *Chiromantis rufescens* based on mtDNA and SNP data

| | UGW | UGE | LG | CON | AEC | NWC |
|---|---|---|---|---|---|---|
| UGW | — | 0.389 | 0.332 | 0.405 | 0.181 | 0.141 |
| UGE | 0.031 | — | 0.183 | 0.266 | 0.105 | 0.079 |
| LG | 0.029 | 0.013 | — | 0.221 | 0.061 | 0.058 |
| CON | 0.032 | 0.027 | 0.027 | — | 0.103 | 0.074 |
| AEC | 0.026 | 0.016 | 0.017 | 0.022 | — | 0.025 |
| NWC | 0.027 | 0.021 | 0.021 | 0.016 | 0.017 | — |

*Note:* Upper diagonal shows population differentiation ($F_{ST}$) from SNP data. Lower diagonal shows average pairwise sequence divergence calculated from the 16S mtDNA data.
Population abbreviations: AEC, atlantic equatorial coastal; CON, congolian; LG, lower guinean; NWC, North-western Congolian; UGE, upper guinean east; UGW, upper guinean west.

**TABLE 4** Analysis of molecular variance (AMOVA) of SNP data from *Chiromantis rufescens*

| Within-population | | Among-population | Among-group |
|---|---|---|---|
| Grouping criteria | % variation, $F_{ST}$ | % variation, $F_{ST}$ | % variation, $F_{ST}$ |
| Dahomey Gap/Cross River | 54.1%, 0.459 | 28.0%, 0.341 | 17.8%, 0.178 |
| Sanaga River barrier | 58.3%, 0.417 | 30.7%, 0.345 | 11.0%, 0.110 |
| **Upper Guinean forest division** | **45.4%, 0.546** | **23.7%, 0.343** | **30.9%, 0.309** |

*Note:* Population assignments assume the $K = 5$ population model. Three alternative population groupings are compared, including Dahomey Gap/Cross River divergence, Sanaga River divergence and a division within the Upper Guinean forest. All $p$-values are significant ($p < .005$). The grouping that maximizes among-group variation is shown in bold.

age for *C. rufescens* is estimated in the Miocene between 5.07 and 9.84 million years ago (median = 7.82 Ma), while the remaining divergence events are within the Pleistocene and end of the Pliocene (Figure 2). The 16S gene tree, estimated jointly with the species tree, supports the monophyly of four populations (UGW, UGE, CON and LG), but LGC is polyphyletic (Figure S6). The species tree topology estimated using the 16S data has weak support (posterior probabilities <0.95) and is mostly congruent with the SNP tree, with the exception of the polyphyly of the LGC populations (Figure 2). The divergence times estimated for the 16S data using secondary fossil calibrations also support a Miocene divergence of the UGW population, but the confidence intervals are much broader (95% HPD = 3.6–11.1) reflecting uncertainty in the data and the priors used for calibrating the tree (Figure 2).

### 3.4 | Demographic models

The 2D demographic modelling results for geographic and phylogenetic population pairs of *C. rufescens* using MOMENTS are presented in Table 5. The top-ranked 2D demographic models selected from among 20 candidate models for pairs of populations that are geographically adjacent to one another all include migration and population size change (Table 5), which is consistent with forest refugia or river barrier diversification. Three epoch models that include the cessation of gene flow in contemporary times are favoured for comparisons of the UGW+UGE and UGE+LG populations. Complex models with different migration patterns across two or three discrete epochs were not selected for LG+LGC or LGC+CON. Instead, these parapatric populations favoured models with asymmetric migration, population size change and secondary contact. The phylogenetic comparisons that lumped populations together to compare sister taxa on the species tree all included asymmetric migration and population size change (Table 5). For the phylogenetic comparison between UGW and all other populations combined, the two models accounting for 100% of the weighted AIC (wAIC) differ by the inclusion–exclusion of secondary contact. Similarly, the other phylogenetic comparisons that included lumped populations also contain multiple top models that differ with respect to secondary contact and three epochs. Graphical representations of the top models and the 2D JSFS projections are shown in Figure 3, and parameter values estimated under the top models (and projection sizes) are in Table S5.

**TABLE 5** Demographic model selection results for *Chiromantis rufescens*

| Populations (comparison type) | | | | |
|---|---|---|---|---|
| **Demographic model(s)** | **Log-likelihood** | ***SD*** | **AIC** | **wAIC** |
| UGW, UGE (geographic) | | | | |
| Secondary contact, symmetric migration, size change, three epoch | −199.6 | 0.37 | 415.1 | 0.79 |
| Secondary contact, asymmetric migration, size change, three epoch | −199.9 | 0.21 | 417.8 | 0.21 |
| UGE, LG (geographic and phylogenetic) | | | | |
| Secondary contact, symmetric migration, size change, three epoch | −294.0 | 0.70 | 604.0 | 0.96 |
| LG, LGC (geographic) | | | | |
| Asymmetric migration, size change | −388.7 | 0.22 | 793.3 | 0.52 |
| Secondary contact, asymmetric migration, size change | −388.8 | 0.10 | 793.5 | 0.46 |
| LGC, CON (geographic) | | | | |
| Secondary contact, asymmetric migration, size change | −377.3 | 0.26 | 770.6 | 0.71 |
| Asymmetric migration, size change | −378.2 | 0.41 | 772.4 | 0.29 |
| LGC, UGE+LG (phylogenetic) | | | | |
| Asymmetric migration, size change | −490.2 | 0.27 | 996.5 | 0.49 |
| Secondary contact, asymmetric migration, size change | −490.5 | 0.21 | 997.0 | 0.37 |
| Secondary contact, asymmetric migration, size change, three epoch | −490.5 | 14.03 | 999.0 | 0.14 |
| CON, LGC+UGE+LG (phylogenetic) | | | | |
| Secondary contact, asymmetric migration, size change, three epoch | −251.1 | 2.64 | 520.1 | 0.52 |
| Secondary contact, asymmetric migration, size change | −252.3 | 1.06 | 520.5 | 0.42 |
| Asymmetric migration, size change | −254.3 | 0.37 | 524.5 | 0.06 |
| UGW, CON+LGC+UGE+LG (phylogenetic) | | | | |
| Asymmetric migration, size change | −193.7 | 0.37 | 403.5 | 0.59 |
| Secondary contact, asymmetric migration, size change | −194.1 | 0.77 | 404.2 | 0.41 |

*Note:* Comparisons include population pairs with neighbouring geographic distributions (geographic) and phylogenetic comparisons guided by the species tree topology (phylogenetic). The models accounting for ≥95% of the cumulative wAIC are shown for each comparison. The standard deviation (*SD*) of the optimized likelihood scores from three replicates runs is shown.

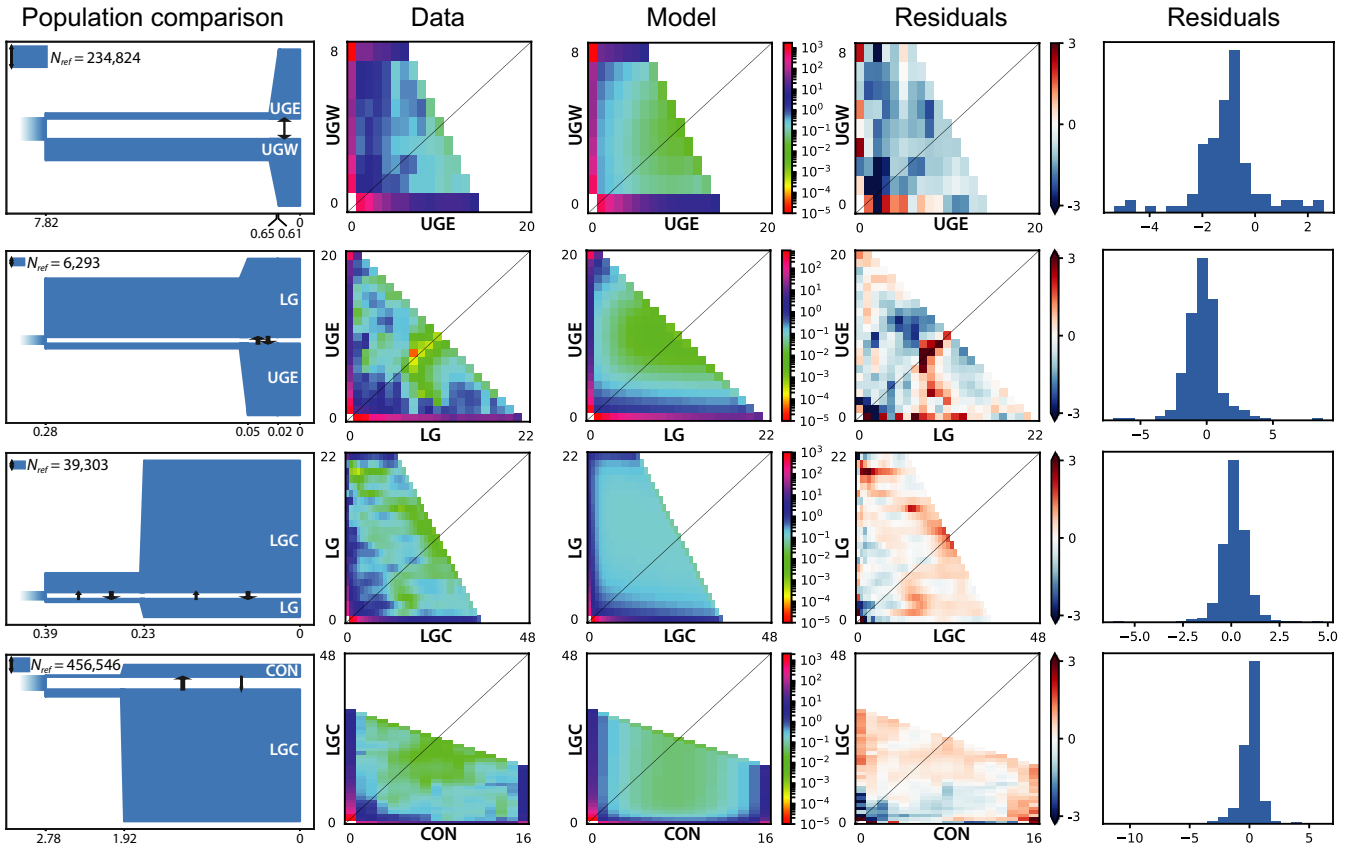


**FIGURE 3** Demographic models selected for *Chiromantis rufescens* populations with neighbouring geographic distributions using two-dimensional site frequency spectrum (2D-SFS). The reference population sizes were scaled to produce population divergence times concordant with the species tree divergence times (Figure 2). The fit between the 2D-SFS model and data is shown with the resulting residuals (positive residuals indicate that the model predicted too many SNPs in that entry)

### 3.5 | Species distribution modelling

The SDM for modern *C. rufescens* had reasonable discrimination ability, with an AUC statistic of 0.82. A "reasonable" AUC in this context is considered to include values from 0.7 to 0.9 (Pearce & Ferrier, 2000). The variables with the most useful and unique information for the model determined by the jackknife analysis included vegetation height, mean diurnal range and precipitation of the driest month. The SDM estimated using projections from the mid-Holocene (6 kybp), the LGM (21 kybp) and the LIG (120 kya) were overlaid to identify shared areas of occurrence and to estimate areas of potential stability (Figure 4). The resulting hindcast or historical model based only on bioclim variables had reasonable discrimination ability (AUC = 0.82). The variables with the highest gain in the model were mean diurnal range and precipitation of the warmest quarter. The projected stability model predicted the regions of bioclimatic stability throughout the Guinean and Congolian forests (Figure 4). The predicted areas of stability overlap spatially with the contemporary locations of populations (Figure 4). There is a close correspondence between the predicted areas of stability and the locations of putative Pleistocene forest refugia based on high species richness or high levels of endemism proposed by Plana (2004) (Figure 4).

## 4 | DISCUSSION

Diversification studies in the Guinean and Congolian rain forests typically place substantial emphasis on the importance of vicariance through isolation in forest refugia, river barriers and ecotones in generating diversity (Moritz et al., 2000; Plana, 2004). Phylogeographic studies provide support for each of these models (Bowie, Fjeldså, Hackett, Bates, & Crowe, 2006; Faye et al., 2016; Gonder et al., 2011; Kirschel et al., 2011). The relative importance of different diversification mechanisms will depend on geography, phylogenetic history and time. The patterns of genetic variation and population divergence that we found in *C. rufescens* are consistent with ecotones, river barriers and forest refugia, depending on the populations considered. The spatio-temporal dynamics of diversification in *C. rufescens* are important, because the species contains at least five populations, some of which likely represent independent evolutionary lineages, spanning multiple important biogeographic areas.

### 4.1 | Phylogeography and systematics

In this study, we provide the first molecular phylogeny for *C. rufescens* to investigate population diversification. Using SNP data, we were able to estimate a resolved and strongly supported species

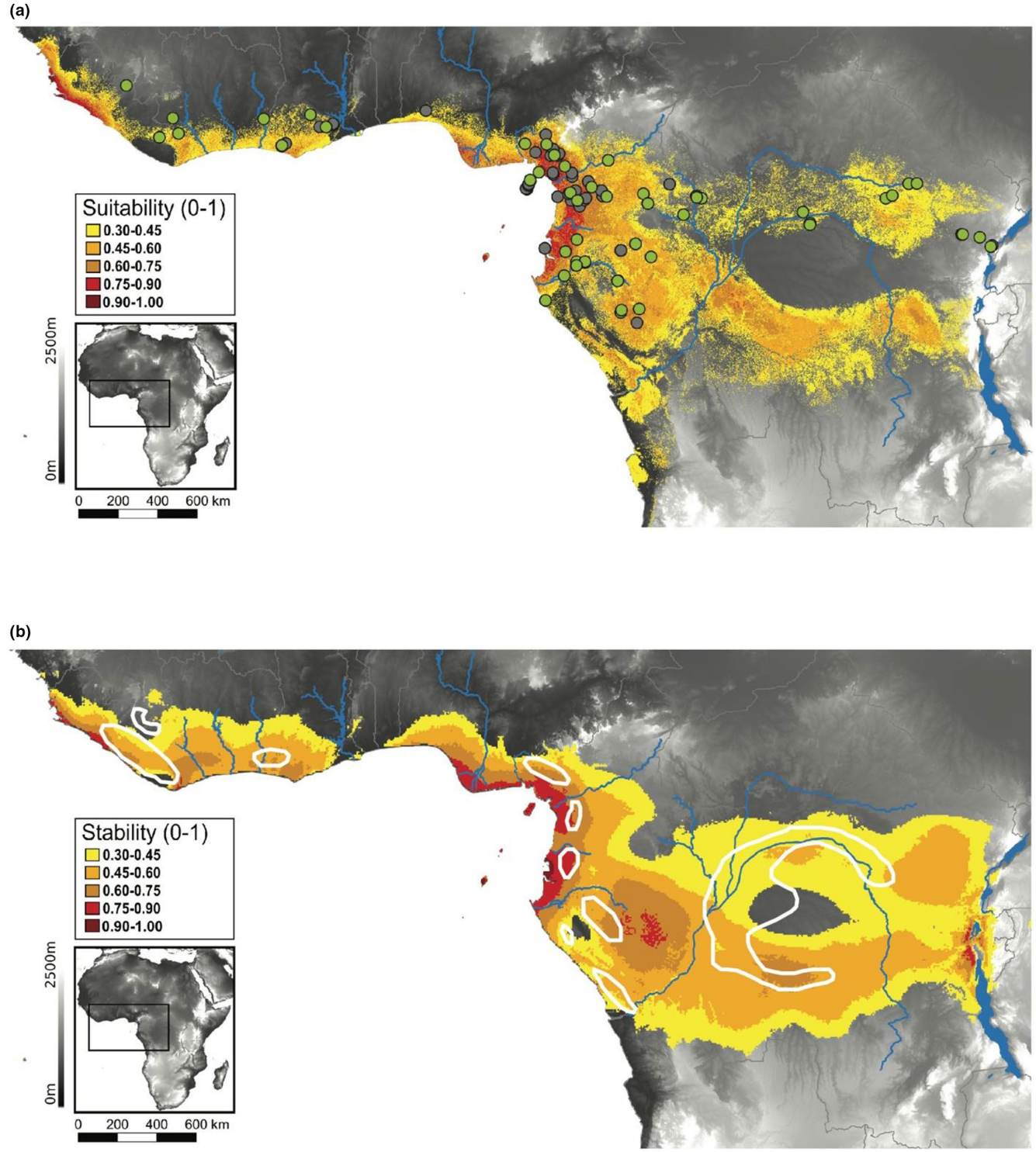


**FIGURE 4** Species distribution models for *Chiromantis rufescens*. (a) SDM estimation of suitability using a combination of bioclimate variables, elevation, vegetation height and distance to rivers. All points shown were used in the models, and points in green were used in genetic analyses. (b) Projected stability model showing the locations of persistent suitable habitat since the last interglacial using only bioclimatic data. Areas with the highest probability of stability are shown in red. The locations of putative Pleistocene forest refugia based on high species richness or high levels of endemism are shown in white (after Plana, 2004)

tree for *C. rufescens* that indicates an early diversification history beginning in the Miocene, followed by more recent diversification in the Pliocene and Pleistocene (Figure 2). The mtDNA data provide an independent source of information for dating the phylogeny. Using secondary fossil calibrations in conjunction with the 16S data also supported diversification starting in the Miocene. The SNP data and mtDNA data both support an initial divergence separating the UGW population from the remainder

of the populations indicates that *C. rufescens* fits the diversification pattern observed in other frogs characterized as colonizers of West Africa. Deep genetic division within the Upper Guinean forest is an emergent pattern seen in multiple frogs that have deeper evolutionary roots in East Africa and sometimes extending into Asia, including *Odontobatrachus* (Barej et al., 2014), *Ptychadena* (Zimkus et al., 2017), and *Amnirana* (Jongsma et al., 2018). This deep genetic divergence also provides further evidence for the evolutionary uniqueness of the western portion of the Upper Guinean forest as a distinct biogeographic region based on amphibian assemblages (Penner et al., 2017, 2011). The UGW population exhibits consistent external morphological differences that distinguish it from all other populations of *C. rufescens*, and a formal description of this new species is currently underway.

### 4.2 | Rivers, refugia and ecotones

Phylogeographic studies integrating demographic and ecological modelling have revealed the importance of multiple mechanisms in driving species diversification in the Guinean and Congolian forests (Faye et al., 2016). Considering historical demography is essential for understanding population diversification, especially in complex landscapes such as those found in the Guineo–Congolian forests (Barratt et al., 2018; Portik et al., 2017). The demographic scenarios that we tested were aimed at determining whether populations diverged with or without gene flow, population size change or secondary contact. These demographic parameters are indicators for the three main diversification models proposed for tropical fauna; the refugia, river and ecotone models (Moritz et al., 2000; Plana, 2004). The diversification history of *C. rufescens* is related to the demographic history of its tropical rain forest habitats, which both support fragmentation and forest refugia models (Duminil et al., 2015; Piñeiro, Dauby, Kaymak, & Hardy, 2017). The forest refugia model is the most likely candidate for driving diversification in *C. rufescens*, because the models favoured population size changes, gene flow, and secondary contact or three epoch models. The forest refugia model includes gene flow for periods of population expansion that brings formerly isolated populations back into contact (Moritz et al., 2000). Ecological modelling predicted areas of stable climate throughout the Guinean and Congolian rain forests during the Pleistocene.

In *C. rufescens*, several of the inferred population divergence events were geographically consistent with river barriers or forest refugia models when considering phylogeographic patterns alone (LG-LGC and LGC-CON; Figure 2). For example, rivers that correspond geographically with inferred population boundaries include the Sanaga River in the Lower Guinea, and the Sassandra, Bandama and Comoé Rivers in the Upper Guinea. The demographic modelling approach was therefore useful for identifying which of these population divergence events were accompanied by population size changes, migration or secondary contact, which are important demographic parameters for discriminating between diversification models. Alternative diversification models make different predictions regarding which demographic parameters are most likely to leave genetic signature during population divergence (Charles et al., 2018; Portik et al., 2017). Under the forest refugia model, forest-obligate species are restricted to fragmented forest patches during glacial maxima (Moritz et al., 2000; Plana, 2004). The expansion and contraction of forest habitats through time can produce population size changes, and facilitate secondary contact between fragmented populations. By contrast, the riverine barrier model predicts high genetic differentiation at river barriers with no expectation for population contraction or expansion. However, the locations of forest refugia are often on opposite sides of rivers, making it difficult to discriminate between the refugia and river models using only phylogeographic patterns and species distribution models (Portik et al., 2017).

The ecotone model of diversification involves parapatric speciation across an ecological gradient (Moritz et al., 2000; Smith, Wayne, Girman, & Bruford, 1997), and therefore population divergence with gene flow and divergent selection are important components of this model. Support for the ecotone model in tropical Africa has mostly come from studies of taxa in Cameroon, where there is evidence of diversification along a well-characterized ecological gradient between forest and savanna habitats (Freedman, Thomassen, Buermann, & Smith, 2010; Smith et al., 2011). We found evidence for a gradient in genetic diversity within the *C. rufescens* population distributed across the AEC and NWC, which fits a pattern of isolation by distance (Figure S4). Genetic differentiation between the *C. rufescens* populations in these forests is weak (Table 3), and the Ogooué River in Gabon only partially separates these two groups (Figure 2). This gradient in genetic differentiation coincides with a west–east gradient in annual rainfall, which decreases from coastal to inland forests in Lower Guinea (Hardy et al., 2013). Several forest plants display genetic divergence along this gradient (Hardy et al., 2013), but it has only been detected in one amphibian (*Hyperolius cinnamomeoventris* species complex; Bell et al. (2017)). *Chiromantis rufescens* is another unique example of genetic differentiation across this under-explored ecological gradient.

### 4.3 | Afro-Asian faunal exchanges

The distinct faunal assemblages that define Africa and southern Asia have long been appreciated by biogeographers (Sclater, 1858; Wallace, 1876). Lönnberg (1929) predicted that two Afro-Asian faunal exchanges occurred in response to climate fluctuations, with the first occurring during the Miocene as forests were globally expanding, and the second exchange during the Pliocene as forests were contracting. Kappelman et al. (2003) also suggested the importance of the Miocene when a major Afro-Asian mammal exchange occurred, primarily as a consequence of the physical connection of Africa and Eurasia via the Arabian Peninsula (Rögl, 1999). A summary of divergence times for taxa with Afro-Asian distributions suggests that many events occurred during the Miocene, but that earlier divergences in the Oligocene and Eocene are also common (Figure S7).

Based on divergence estimates obtained using the mtDNA phylogeny (Figure S6), the split between African and Asian *Chiromantis* is estimated at 27.1 MA (18.3–35.1 MA). Among amphibians,

*Chiromantis* and *Amnirana* both have Afro-Asian divergences that could have occurred as early as the Oligocene (Figure S7). If accurate, these dates predate the Miocene exchange, and push the earliest divergence as far back as the middle Eocene (45 MA). This divergence time estimate needs to be investigated with more loci, extensive sampling of *Chiromantis*, and additional fossil evidence as it becomes available. Several other vertebrates also share early Afro-Asian divergences that span the Eocene and Oligocene (Figure S7). These include examples from primates (Pozzi et al., 2014), carnivores (Gaubert & Cordeiro-Estrela, 2006), snakes (Wüster et al., 2007), lizards (Dowell, Buffrénil, Kolokotronis, & Hekkala, 2015) and birds (Barker, Cibois, Schikler, Feinstein, & Cracraft, 2004; Moyle, Chesser, Prum, Schikler, & Cracraft, 2006). The Miocene may have been a high point for biotic exchanges between Africa and Asia, but by this time *C. rufescens* was already diversifying in West Africa, specifically in the Upper Guinean forest (Figure 2).

## ACKNOWLEDGEMENTS

We thank the respective West and Central African authorities for research, access and collection and export permits, as well as our many guides and field assistants. We thank Kevin Epperly for collecting the ddRADseq data, and Sergei Drovetski for collecting the mtDNA data in the L.A.B. facilities of the National Museum of Natural History (NMNH). For tissue loans, we thank Sharon Birks (Burke Museum of Natural History and Culture), Bryan Stuart (North Carolina Museum of Natural Sciences), Jens Vindum and Lauren Scheinberg (California Academy of Sciences), Brandi Coyner and Cameron Siler (Sam Noble Museum), Carol Spencer and Jim McGuire (Museum of Vertebrate Zoology). Field work in West Africa was supported by the German Ministry for Education and Research (BMBF) through the BIOTA-West project (funding number 01LC0617J) and the German Science Foundation (DFG VE 183/4-1 & RO 306/1-2). VG was supported by the Czech Science Foundation (GACR 15-13415Y), and Ministry of Culture of the Czech Republic (DKRVO 2018/14 and 2019–2023/6.VII.a, National Museum, 00023272), and thank B.G. Badjedjea, M. Dolinay, M. Jirku, O. Kopecky, D. Modry and A.G. Zassi-Boulou for assistance in the field or additional material. Field work in Democratic Republic of the Congo by EG was supported by a National Geographic Research and Exploration Grant (no. 8556-08), and the US National Science Foundation (DEB-1145459). This work used the Vincent J. Coates Genomics Sequencing Laboratory at UC Berkeley, supported by NIH S10 OD018174 Instrumentation Grant. We thank two anonymous reviewers and the Associate Editor, Krystal Tolley, for helpful comments on the manuscript.

## DATA AVAILABILITY STATEMENT

Demultiplexed ddRADseq data are deposited at the NCBI SRA (PRJNA528800). The 16S sequences are deposited at GenBank (accession numbers MK789304–MK789428). Additional data files used for SNP and mtDNA data analyses are available on Dryad (https://doi.org/10.5061/dryad.bm8r6pr).

## REFERENCES

Barej, M. F., Schmitz, A., Günther, R., Loader, S. P., Mahlow, K., & Rödel, M.-O. (2014). The first endemic West African vertebrate family–a new anuran family highlighting the uniqueness of the Upper Guinean biodiversity hotspot. *Frontiers in Zoology*, *11*, 8. https://doi.org/10.1186/1742-9994-11-8

Barej, M. F., Schmitz, A., Menegon, M., Hillers, A., Hinkel, H., Boehme, W., & Roedel, M.-O. (2011). Dusted off–the African *Amietophrynus superciliaris*-species complex of giant toads. *Zootaxa*, *2772*, 1–32. https://doi.org/10.11646/zootaxa.2772.1.1

Barker, F. K., Cibois, A., Schikler, P., Feinstein, J., & Cracraft, J. (2004). Phylogeny and diversification of the largest avian radiation. *Proceedings of the National Academy of Sciences USA*, *101*, 11040–11045. https://doi.org/10.1073/pnas.0401892101

Barratt, C. D., Bwong, B. A., Jehle, R., Liedtke, H. C., Nagel, P., Onstein, R. E., … Loader, S. P. (2018). Vanishing refuge? testing the forest refuge hypothesis in coastal East Africa using genome-wide sequence data for seven amphibians. *Molecular Ecology*, *27*, 4289–4308. https://doi.org/10.1111/mec.14862

Bell, R. C., Parra, J. L., Badjedjea, G., Barej, M. F., Blackburn, D. C., Burger, M., … Zamudio, K. R. (2017). Idiosyncratic responses to climate-driven forest fragmentation and marine incursions in reed frogs from Central Africa and the Gulf of Guinea Islands. *Molecular Ecology*, *26*, 5223–5244. https://doi.org/10.1111/mec.14260

Boria, R. A., Olson, L. E., Goodman, S. M., & Anderson, R. P. (2014). Spatial filtering to reduce sampling bias can improve the performance of ecological niche models. *Ecological Modelling*, *275*, 73–77. https://doi.org/10.1016/j.ecolmodel.2013.12.012

Bouckaert, R. R. (2010). DensiTree: Making sense of sets of trees. *Bioinformatics*, *26*, 1372–1373.

Bouckaert, R., Heled, J., Kühnert, D., Vaughan, T., Wu, C.-H., Xie, D., … Drummond, A. J. (2014). BEAST 2: A software platform for Bayesian evolutionary analysis. *PLoS Computational Biology*, *10*, e1003537. https://doi.org/10.1371/journal.pcbi.1003537

Bowie, R. C., Fjeldså, J., Hackett, S. J., Bates, J. M., & Crowe, T. M. (2006). Coalescent models reveal the relative roles of ancestral polymorphism, vicariance, and dispersal in shaping phylogeographical structure of an African montane forest robin. *Molecular Phylogenetics and Evolution*, *38*, 171–188. https://doi.org/10.1016/j.ympev.2005.06.001

Brown, J. L. (2014). SDMtoolbox: A python-based GIS toolkit for landscape genetic, biogeographic and species distribution model analyses. *Methods in Ecology and Evolution*, *5*, 694–700. https://doi.org/10.1111/2041-210X.12200

Brown, J. L., Bennett, J. R., & French, C. M. (2017). SDMtoolbox 2.0: The next generation Python-based GIS toolkit for landscape genetic, biogeographic and species distribution model analyses. *PeerJ*, *5*, e4095.

Bryant, D., Bouckaert, R., Felsenstein, J., Rosenberg, N. A., & RoyChoudhury, A. (2012). Inferring species trees directly from biallelic genetic markers: Bypassing gene trees in a full coalescent analysis. *Molecular Biology and Evolution*, *29*, 1917–1932. https://doi.org/10.1093/molbev/mss086

Burnham, K. P., & Anderson, D. R. (2003). *Model selection and multimodel inference: A practical information-theoretic approach*. (2nd ed.). New York, NY: Springer.

Charles, K. L., Bell, R. C., Blackburn, D. C., Burger, M., Fujita, M. K., Gvoždík, V., … Portik, D. M. (2018). Sky, sea, and forest islands: Diversification in the African leaf-folding frog *Afrixalus paradorsalis* (Anura: Hyperoliidae) of the Lower Guineo-Congolian rainforest. *Journal of Biogeography*, *45*, 1781–1794.

Coe, M. J. (1967). Co-operation of three males in nest construction by *Chiromantis rufescens* Gunther (Amphibia: Rhacophoridae). *Nature*, *214*, 112. https://doi.org/10.1038/214112b0

Coe, M. (1974). Observations on the ecology and breeding biology of the genus *Chiromantis* (Amphibia: Rhacophoridae). *Journal of Zoology*, *172*, 13–34. https://doi.org/10.1111/j.1469-7998.1974.tb04091.x

Constable, H., Guralnick, R., Wieczorek, J., Spencer, C., Peterson, A. T., Committee, V. S., et al. (2010). VertNet: A new model for biodiversity data sharing. *PLoS Biology*, *8*, e1000309. https://doi.org/10.1371/journal.pbio.1000309

Danecek, P., Auton, A., Abecasis, G., Albers, C. A., Banks, E., DePristo, M. A., … Durbin, R. (2011). The variant call format and VCFtools. *Bioinformatics*, *27*, 2156–2158. https://doi.org/10.1093/bioinformatics/btr330

Darriba, D., Taboada, G. L., Doallo, R., & Posada, D. (2012). jModelTest 2: More models, new heuristics and parallel computing. *Nature Methods*, *9*, 772. https://doi.org/10.1038/nmeth.2109

Devitt, T. J., Devitt, S. E. C., Hollingsworth, B. D., McGuire, J. A., & Moritz, C. (2013). Montane refugia predict population genetic structure in the large-blotched *Ensatina* salamander. *Molecular Ecology*, *22*, 1650–1665. https://doi.org/10.1111/mec.12196

Dowell, S. A., de Buffrénil, V., Kolokotronis, S.-O., & Hekkala, E. R. (2015). Fine-scale genetic analysis of the exploited nile monitor (*Varanus niloticus*) in Sahelian Africa. *BMC Genetics*, *16*, 32. https://doi.org/10.1186/s12863-015-0188-x

Dowell, S. A., Portik, D. M., de Buffrénil, V., Ineich, I., Greenbaum, E., Kolokotronis, S.-O., & Hekkala, E. R. (2016). Molecular data from contemporary and historical collections reveal a complex story of cryptic diversification in the *Varanus (Polydaedalus) niloticus* species group. *Molecular Phylogenetics and Evolution*, *94*, 591–604. https://doi.org/10.1016/j.ympev.2015.10.004

Duminil, J., Mona, S., Mardulyn, P., Doumenge, C., Walmacq, F., Doucet, J.-L., & Hardy, O. J. (2015). Late Pleistocene molecular dating of past population fragmentation and demographic changes in African rain forest tree species supports the forest refuge hypothesis. *Journal of Biogeography*, *42*, 1443–1454. https://doi.org/10.1111/jbi.12510

Dupont, L. M., Jahns, S., Marret, F., & Ning, S. (2000). Vegetation change in equatorial West Africa: Time-slices for the last 150 ka. *Palaeogeography, Palaeoclimatology, Palaeoecology*, *155*, 95–122. https://doi.org/10.1016/S0031-0182(99)00095-4

Earl, D. A., & vonHoldt, B. M. (2012). STRUCTURE HARVESTER: A website and program for visualizing STRUCTURE output and implementing the Evanno method. *Conservation Genetics Resources*, *4*, 359–361. https://doi.org/10.1007/s12686-011-9548-7

Eaton, D. A. (2014). PyRAD: Assembly of de novo RADseq loci for phylogenetic analyses. *Bioinformatics*, *30*, 1844–1849. https://doi.org/10.1093/bioinformatics/btu121

Edgar, R. C. (2010). Search and clustering orders of magnitude faster than BLAST. *Bioinformatics*, *26*, 2460–2461. https://doi.org/10.1093/bioinformatics/btq461

Farr, T. G., Rosen, P. A., Caro, E., Crippen, R., Duren, R., Hensley, S., … Alsdorf, D. (2007). The shuttle radar topography mission. *Reviews of Geophysics*, *45*, 1–33. https://doi.org/10.1029/2005RG000183

Faye, A., Deblauwe, V., Mariac, C., Richard, D., Sonké, B., Vigouroux, Y., & Couvreur, T. (2016). Phylogeography of the genus *Podococcus* (Palmae/Arecaceae) in Central African rain forests: Climate stability predicts unique genetic diversity. *Molecular Phylogenetics and Evolution*, *105*, 126–138. https://doi.org/10.1016/j.ympev.2016.08.005

Fjeldså, J., & Bowie, R. C. (2008). New perspectives on the origin and diversification of Africa's forest avifauna. *African Journal of Ecology*, *46*, 235–247. https://doi.org/10.1111/j.1365-2028.2008.00992.x

Freedman, A. H., Thomassen, H. A., Buermann, W., & Smith, T. B. (2010). Genomic signals of diversification along ecological gradients in a tropical lizard. *Molecular Ecology*, *19*, 3773–3788. https://doi.org/10.1111/j.1365-294X.2010.04684.x

Gaubert, P., & Cordeiro-Estrela, P. (2006). Phylogenetic systematics and tempo of evolution of the Viverrinae (Mammalia, Carnivora, Viverridae) within feliformians: Implications for faunal exchanges between Asia and Africa. *Molecular Phylogenetics and Evolution*, *41*, 266–278. https://doi.org/10.1016/j.ympev.2006.05.034

Gaubert, P., Njiokou, F., Ngua, G., Afiademanyo, K., Dufour, S., Malekani, J., … Antunes, A. (2016). Phylogeography of the heavily poached African common pangolin (Pholidota, *Manis tricuspis*) reveals six cryptic lineages as traceable signatures of Pleistocene diversification. *Molecular Ecology*, *25*, 5975–5993.

Gonder, M. K., Locatelli, S., Ghobrial, L., Mitchell, M. W., Kujawski, J. T., Lankester, F. J., … Tishkoff, S. A. (2011). Evidence from Cameroon reveals differences in the genetic structure and histories of chimpanzee populations. *Proceedings of the National Academy of Sciences*, *108*, 4766–4771. https://doi.org/10.1073/pnas.1015422108

Greenbaum, E., Portillo, F., Jackson, K., & Kusamba, C. (2015). A phylogeny of Central African *Boaedon* (Serpentes: Lamprophiidae), with the description of a new cryptic species from the Albertine Rift. *African Journal of Herpetology*, *64*, 18–38.

Gutenkunst, R. N., Hernandez, R. D., Williamson, S. H., & Bustamante, C. D. (2009). Inferring the joint demographic history of multiple populations from multidimensional SNP frequency data. *PLoS Genetics*, *5*, e1000695. https://doi.org/10.1371/journal.pgen.1000695

Günther, A. C. L. G. (1869). First account of species of tailless batrachians added to the collection of the British Museum. *Proceedings of the Zoological Society of London*, *1868*, 478–490.

Hamilton, A. C., & Taylor, D. (1991). History of climate and forests in tropical Africa during the last 8 million years. In N. Myers (Ed.) *Tropical forests and climate* (pp 65–78). Dordrecht: Springer.

Hardy, O. J., Born, C., Budde, K., Daïnou, K., Dauby, G., Duminil, J., … Poncet, V. (2013). Comparative phylogeography of African rain forest trees: A review of genetic signatures of vegetation history in the Guineo-Congolian region. *Comptes Rendus Geoscience*, *345*, 284–296. https://doi.org/10.1016/j.crte.2013.05.001

Hasegawa, M., Kishino, H., & Yano, T.-A. (1985). Dating of the human-ape splitting by a molecular clock of mitochondrial DNA. *Journal of Molecular Evolution*, *22*, 160–174. https://doi.org/10.1007/BF02101694

Hijmans, R. J. (2012). Cross-validation of species distribution models: Removing spatial sorting bias and calibration with a null model. *Ecology*, *93*, 679–688. https://doi.org/10.1890/11-0826.1

Hijmans, R. J., Cameron, S. E., Parra, J. L., Jones, P. G., & Jarvis, A. (2005). Very high resolution interpolated climate surfaces for global land areas. *International Journal of Climatology*, *25*, 965–1978. https://doi.org/10.1002/joc.1276

Hughes, D. F., Kusamba, C., Behangana, M., & Greenbaum, E. (2017). Integrative taxonomy of the Central African forest chameleon, *Kinyongia adolfifriderici* (Sauria: Chamaeleonidae), reveals underestimated species diversity in the Albertine Rift. *Zoological Journal of the Linnean Society*, *181*, 400–438. https://doi.org/10.1093/zoolinnean/zlx005

Jablonski, D., Roy, K., & Valentine, J. W. (2006). Out of the tropics: Evolutionary dynamics of the latitudinal diversity gradient. *Science*, *314*, 102–106. https://doi.org/10.1126/science.1130880

Jombart, T., & Ahmed, I. (2011). adegenet 1.3-1: New tools for the analysis of genome-wide SNP data. *Bioinformatics*, *27*, 3070–3071.

Jombart, T., Devillard, S., & Balloux, F. (2010). Discriminant analysis of principal components: A new method for the analysis of genetically structured populations. *BMC Genetics*, *11*, 94. https://doi.org/10.1186/1471-2156-11-94

Jongsma, G. F. M., Barej, M. F., Barratt, C. D., Burger, M., Conradie, W., Ernst, R., … Blackburn, D. C. (2018). Diversity and biogeography of frogs in the genus *Amnirana* (Anura: Ranidae) across sub-Saharan

Africa. *Molecular Phylogenetics and Evolution*, *120*, 274–285. https://doi.org/10.1016/j.ympev.2017.12.006

Jouganous, J., Long, W., Ragsdale, A. P., & Gravel, S. (2017). Inferring the joint demographic history of multiple populations: Beyond the diffusion approximation. *Genetics*, *206*, 1549–1567.

Kappelman, J., Rasmussen, D. T., Sanders, W. J., Feseha, M., Bown, T., Copeland, P., … Winkler, A. (2003). Oligocene mammals from Ethiopia and faunal exchange between Afro-Arabia and Eurasia. *Nature*, *426*, 549. https://doi.org/10.1038/nature02102

Katoh, K., Kuma, K.-I., Toh, H., & Miyata, T. (2005). MAFFT version 5: Improvement in accuracy of multiple sequence alignment. *Nucleic Acids Research*, *33*, 511–518. https://doi.org/10.1093/nar/gki198

Kirschel, A. N., Slabbekoorn, H., Blumstein, D. T., Cohen, R. E., de Kort, S. R., Buermann, W., & Smith, T. B. (2011). Testing alternative hypotheses for evolutionary diversification in an African songbird: Rainforest refugia versus ecological gradients. *Evolution*, *65*, 3162–3174. https://doi.org/10.1111/j.1558-5646.2011.01386.x

Larson, T. R., Castro, D., Behangana, M., & Greenbaum, E. (2016). Evolutionary history of the river frog genus *Amietia* (Anura: Pyxicephalidae) reveals extensive diversification in Central African highlands. *Molecular Phylogenetics and Evolution*, *99*, 168–181. https://doi.org/10.1016/j.ympev.2016.03.017

Leaché, A. D., & Fujita, M. K. (2010). Bayesian species delimitation in West African forest geckos (*Hemidactylus fasciatus*). *Proceedings of the Royal Society of London B: Biological Sciences*, *277*:3071–3077. https://doi.org/10.1098/rspb.2010.0662

Leaché, A. D., Grummer, J. A., Miller, M., Krishnan, S., Fujita, M. K., Böhme, W., … Chirio, L., et al. (2017). Bayesian inference of species diffusion in the West African *Agama agama* species group (Reptilia, Agamidae). *Systematics and Biodiversity*, *15*, 192–203.

Lee, D.-C., Halliday, A. N., Fitton, J. G., & Poli, G. (1994). Isotopic variations with distance and time in the volcanic islands of the Cameroon line: Evidence for a mantle plume origin. *Earth and Planetary Science Letters*, *123*, 119–138. https://doi.org/10.1016/0012-821X(94)90262-3

Li, J.-T., Che, J., Murphy, R. W., Zhao, H., Zhao, E.-M., Rao, D.-Q., & Zhang, Y.-P. (2009). New insights to the molecular phylogenetics and generic assessment in the Rhacophoridae (Amphibia: Anura) based on five nuclear and three mitochondrial genes, with comments on the evolution of reproduction. *Molecular Phylogenetics and Evolution*, *53*, 509–522. https://doi.org/10.1016/j.ympev.2009.06.023

Lönnberg, E. (1929). The development and distribution of the African fauna in connection with and depending upon climatic changes. *Arkiv för Zoologi*, 21 A, 1-33.

Lynch, M. (2010). Rate, molecular spectrum, and consequences of human mutation. *Proceedings of the National Academy of Sciences*, *107*, 961–968. https://doi.org/10.1073/pnas.0912629107

Maley, J. (1991). The African rain forest vegetation and palaeoenvironments during late Quaternary. *Climatic Change*, *19*, 79–98.

Marks, B. D. (2010). Are lowland rainforests really evolutionary museums? phylogeography of the green hylia (*Hylia prasina*) in the Afrotropics. *Molecular Phylogenetics and Evolution*, *55*, 178–184. https://doi.org/10.1016/j.ympev.2009.10.027

Meegaskumbura, M., Senevirathne, G., Biju, S., Garg, S., Meegaskumbura, S., Pethiyagoda, R., … Schneider, C. J. (2015). Patterns of reproductive-mode evolution in Old World tree frogs (Anura, Rhacophoridae). *Zoologica Scripta*, *44*, 509–522. https://doi.org/10.1111/zsc.12121

Meirmans, P. G., & Van Tienderen, P. H. (2004). GENOTYPE and GENODIVE: Two programs for the analysis of genetic diversity of asexual organisms. *Molecular Ecology Resources*, *4*, 792–794. https://doi.org/10.1111/j.1471-8286.2004.00770.x

Menegon, M., Loader, S., Marsden, S., Branch, W., Davenport, T., & Ursenbacher, S. (2014). The genus *Atheris* (Serpentes: Viperidae) in East Africa: Phylogeny and the role of rifting and climate in shaping the current pattern of species diversity. *Molecular Phylogenetics and Evolution*, *79*, 12–22. https://doi.org/10.1016/j.ympev.2014.06.007

Moritz, C., Patton, J., Schneider, C., & Smith, T. (2000). Diversification of rainforest faunas: An integrated molecular approach. *Annual Review of Ecology and Systematics*, *31*, 533–563. https://doi.org/10.1146/annurev.ecolsys.31.1.533

Moyle, R. G., Chesser, R. T., Prum, R. O., Schikler, P., & Cracraft, J. (2006). Phylogeny and evolutionary history of Old World suboscine birds (Aves: *Eurylaimides*). *American Museum Novitates*, *2006*(3544), 1–22. https://doi.org/10.1206/0003-0082(2006)3544[1:PAEHOO]2.0.CO;2

Myers, N., Mittermeier, R. A., Mittermeier, C. G., Da Fonseca, G. A., & Kent, J. (2000). Biodiversity hotspots for conservation priorities. *Nature*, *403*, 853–858. https://doi.org/10.1038/35002501

Nei, M. (1978). Estimation of average heterozygosity and genetic distance from a small number of individuals. *Genetics*, *89*, 583–590.

Ogilvie, H. A., Bouckaert, R. R., & Drummond, A. J. (2017). StarBEAST2 brings faster species tree inference and accurate estimates of substitution rates. *Molecular Biology and Evolution*, *34*, 2101–2114. https://doi.org/10.1093/molbev/msx126

Olson, D. M., & Dinerstein, E. (2002). The Global 200: Priority ecoregions for global conservation. *Annals of the Missouri Botanical Garden*, 89(2), Spring, 199–224. https://doi.org/10.2307/3298564

Onn, C. K., Grismer, L. L., & Brown, R. M. (2018). Comprehensive multilocus phylogeny of Old World tree frogs (Anura: Rhacophoridae) reveals taxonomic uncertainties and potential cases of over- and underestimation of species diversity. *Molecular Phylogenetics and Evolution*, *127*, 1010–1019.

Palumbi, S. R. (1996). Nucleic acids II: the polymerase chain reaction. In D. M. Hillis, C. Moritz, & B. K. Mable (Eds.). *Molecular systematics* (pp 205–247). Sunderland, MA: Sinauer & Associates Inc.

Pearce, J., & Ferrier, S. (2000). Evaluating the predictive performance of habitat models developed using logistic regression. *Ecological Modelling*, *133*, 225–245. https://doi.org/10.1016/S0304-3800(00)00322-7

Penner, J., Adum, G. B., McElroy, M. T., Doherty-Bone, T., Hirschfeld, M., Sandberger, L., … Rödel, M.-O. (2013). West Africa-a safe haven for frogs? a sub-continental assessment of the chytrid fungus (*Batrachochytrium dendrobatidis*). *PLoS ONE*, *8*, e56236. https://doi.org/10.1371/journal.pone.0056236

Penner, J., Augustin, M., & Rödel, M.-O. (2017). Modelling the spatial baseline for amphibian conservation in West Africa. *Acta Oecologica*, in press.

Penner, J., Wegmann, M., Hillers, A., Schmidt, M., & Rödel, M.-O. (2011). A hotspot revisited–a biogeographical analysis of West African amphibians. *Diversity and Distributions*, *17*, 1077–1088. https://doi.org/10.1111/j.1472-4642.2011.00801.x

Peterson, B. K., Weber, J. N., Kay, E. H., Fisher, H. S., & Hoekstra, H. E. (2012). Double digest RADseq: An inexpensive method for de novo SNP discovery and genotyping in model and non-model species. *PLoS ONE*, *7*, e37135. https://doi.org/10.1371/journal.pone.0037135

Phillips, S. J., Anderson, R. P., & Schapire, R. E. (2006). Maximum entropy modeling of species geographic distributions. *Ecological Modelling*, *190*, 231–259. https://doi.org/10.1016/j.ecolmodel.2005.03.026

Piñeiro, R., Dauby, G., Kaymak, E., & Hardy, O. J. (2017). Pleistocene population expansions of shade-tolerant trees indicate fragmentation of the African rainforest during the Ice Ages. *Proceedings of the Royal Society B: Biological Sciences*, *284*, 20171800. https://doi.org/10.1098/rspb.2017.1800

Plana, V. (2004). Mechanisms and tempo of evolution in the African Guineo-Congolian rainforest. *Philosophical Transactions of the Royal Society B: Biological Sciences*, *359*, 1585–1594. https://doi.org/10.1098/rstb.2004.1535

Portik, D. M., Leaché, A. D., Rivera, D., Barej, M. F., Burger, M., Hirschfeld, M., … Fujita, M. K. (2017). Evaluating mechanisms of diversification in a Guineo-Congolian forest frog using demographic model selection. *Molecular Ecology*, *26*, 5245–5263.

Portillo, F., Branch, W. R., Conradie, W., Rödel, M.-O., Penner, J., Barej, M. F., … Greenbaum, E. (2018). Phylogeny and biogeography of the African burrowing snake subfamily Aparallactinae (Squamata: Lamprophiidae). *Molecular Phylogenetics and Evolution*, *127*, 288–303.

Pozzi, L., Hodgson, J. A., Burrell, A. S., Sterner, K. N., Raaum, R. L., & Disotell, T. R. (2014). Primate phylogenetic relationships and divergence dates inferred from complete mitochondrial genomes. *Molecular Phylogenetics and Evolution*, *75*, 165–183. https://doi.org/10.1016/j.ympev.2014.02.023

Pritchard, J. K., Stephens, M., & Donnelly, P. (2000). Inference of population structure using multilocus genotype data. *Genetics*, *155*, 945–959.

Pyron, R. A., & Wiens, J. J. (2013). Large-scale phylogenetic analyses reveal the causes of high tropical amphibian diversity. *Proceedings of the Royal Society B: Biological Sciences*, *280*, 20131622. https://doi.org/10.1098/rspb.2013.1622

Radosavljevic, A., & Anderson, R. P. (2014). Making better Maxent models of species distributions: Complexity, overfitting and evaluation. *Journal of Biogeography*, *41*, 629–643.

Rödel, M.-O., Range, F., Seppänen, J.-T., & Noë, R. (2002). Caviar in the rain forest: Monkeys as frog-spawn predators in Taï National Park, Ivory Coast. *Journal of Tropical Ecology*, *18*, 289–294. https://doi.org/10.1017/S0266467402002195

Rögl, F. (1999). Mediterranean and Paratethys. facts and hypotheses of an Oligocene to Miocene paleogeography (short overview). *Geologica Carpathica*, *50*, 339–349.

Roll, U., Geffen, E., & Yom-Tov, Y. (2015). Linking vertebrate species richness to tree canopy height on a global scale. *Global Ecology and Biogeography*, *24*, 814–825. https://doi.org/10.1111/geb.12325

Rosenberg, N. A. (2004). DISTRUCT: A program for the graphical display of population structure. *Molecular Ecology Resources*, *4*, 137–138. https://doi.org/10.1046/j.1471-8286.2003.00566.x

Salzmann, U., & Hoelzmann, P. (2005). The Dahomey Gap: An abrupt climatically induced rain forest fragmentation in West Africa during the late Holocene. *The Holocene*, *15*, 190–199. https://doi.org/10.1191/0959683605hl799rp

Scally, A., & Durbin, R. (2012). Revising the human mutation rate: Implications for understanding human evolution. *Nature Reviews Genetics*, *13*, 745. https://doi.org/10.1038/nrg3295

Sclater, P. L. (1858). On the general geographical distribution of the members of the class Aves. *Journal of the Proceedings of the Linnean Society of London. Zoology*, *2*, 130–136.

Shcheglovitova, M., & Anderson, R. P. (2013). Estimating optimal complexity for ecological niche models: A jackknife approach for species with small sample sizes. *Ecological Modelling*, *269*, 9–17. https://doi.org/10.1016/j.ecolmodel.2013.08.011

Simard, M., Pinto, N., Fisher, J. B., & Baccini, A. (2011). Mapping forest canopy height globally with spaceborne lidar. *Journal of Geophysical Research: Biogeosciences*, *116*(G4). https://doi.org/10.1029/2011JG001708

Smith, T. B., Thomassen, H. A., Freedman, A. H., Sehgal, R. N. M., Buermann, W., Saatchi, S., … Wayne, R. K. (2011). Patterns of divergence in the olive sunbird *Cyanomitra olivacea* (Aves: Nectariniidae) across the African rainforest–savanna ecotone. *Biological Journal of the Linnean Society*, *103*, 821–835. https://doi.org/10.1111/j.1095-8312.2011.01674.x

Smith, T. B., Wayne, R. K., Girman, D. J., & Bruford, M. W. (1997). A role for ecotones in generating rainforest biodiversity. *Science*, *276*, 1855–1857. https://doi.org/10.1126/science.276.5320.1855

Veloz, S. D. (2009). Spatially autocorrelated sampling falsely inflates measures of accuracy for presence-only niche models. *Journal of Biogeography*, *36*, 2290–2299. https://doi.org/10.1111/j.1365-2699.2009.02174.x

Vences, M., Vieites, D. R., Glaw, F., Brinkmann, H., Kosuch, J., Veith, M., & Meyer, A. (2003). Multiple overseas dispersal in amphibians. *Proceedings of the Royal Society of London. Series B: Biological Sciences*, *270*, 2435–2442. https://doi.org/10.1098/rspb.2003.2516

Wallace, A. R. (1876). The geographical distribution of animals; with a study of the relations of living and extinct faunas as elucidating the past changes of the earth's surface (Vol. 2). London: Macmillan & Co.

Weir, B. S., & Cockerham, C. C. (1984). Estimating F-statistics for the analysis of population structure. *Evolution*, *38*, 1358–1370.

White, F. (1979). The Guineo-Congolian Region and its relationships to other phytochoria. *Bulletin du Jardin Botanique National de Belgique/ Bulletin van de Nationale Plantentuin van Belgie*, 49(1/2), 11–55.

Wüster, W., Crookes, S., Ineich, I., Mané, Y., Pook, C. E., Trape, J.-F., & Broadley, D. G. (2007). The phylogeny of cobras inferred from mitochondrial DNA sequences: Evolution of venom spitting and the phylogeography of the African spitting cobras (Serpentes: Elapidae: *Naja nigricollis* complex). *Molecular Phylogenetics and Evolution*, *45*, 437–453. https://doi.org/10.1016/j.ympev.2007.07.021

Yannic, G., Pellissier, L., Ortego, J., Lecomte, N., Couturier, S., Cuyler, C., … Côté, S. D. (2014). Genetic diversity in caribou linked to past and future climate change. *Nature Climate Change*, *4*, 132–137. https://doi.org/10.1038/nclimate2074

Yu, G., Rao, D., Zhang, M., & Yang, J. (2009). Re-examination of the phylogeny of Rhacophoridae (Anura) based on mitochondrial and nuclear DNA. *Molecular Phylogenetics and Evolution*, *50*, 571–579. https://doi.org/10.1016/j.ympev.2008.11.023

Yuan, Z.-Y., Zhang, B.-L., Raxworthy, C. J., Weisrock, D. W., Hime, P. M., Jin, J.-Q., … Prendini, E. (2019). Natatanuran frogs used the Indian Plate to step-stone disperse and radiate across the Indian Ocean. *National Science Review*, *6*, 10–14.

Zimkus, B. M., Lawson, L. P., Barej, M. F., Barratt, C. D., Channing, A., Dash, K. M., … Lötters, S. (2017). Leapfrogging into new territory: How mascarene ridged frogs diversified across Africa and Madagascar to maintain their ecological niche. *Molecular Phylogenetics and Evolution*, *106*, 254–269. https://doi.org/10.1016/j.ympev.2016.09.018

## BIOSKETCH

**Adam D. Leaché** is an Associate Professor of Biology and Curator of Herpetology and Genetic Resources at the Burke Museum of Natural History and Culture at the University of Washington. He studies phylogenetics, phylogeography and species delimitation.

Author contributions: A.D.L., M.K.F and D.M.P. conceived the study. All authors collected specimens and contributed to manuscript writing. A.D.L., D.M.P., D.R., J.P., R.C.B and M.K.F. analysed the data.

## SUPPORTING INFORMATION

Additional supporting information may be found online in the Supporting Information section at the end of the article.

**How to cite this article:** Leaché AD, Portik DM, Rivera D, et al. Exploring rain forest diversification using demographic model testing in the African foam-nest treefrog *Chiromantis rufescens*. *J Biogeogr*. 2019;00:1–16. https://doi.org/10.1111/jbi.13716